DOI: 10.1002/chem.200500773

Self-Organizing Properties of Monosubstituted Sucrose Fatty Acid Esters: The Effects of Chain Length and Unsaturation

Valérie Molinier,[a, d] Paul J. J. Kouwer,[c, e] Juliette Fitremann,[a, f] Alain Bouchu,[a] Grahame Mackenzie,[c] Yves Queneau,*[a] and John W. Goodby*[b]

Abstract: Three families of mono-substituted sucrose fatty acid esters were prepared by enzymatic and classical synthetic procedures, and their self-assembly and self-organizational properties were investigated by thermal polarised light microscopy, differential scanning calorimetry and X-ray diffraction. The properties were evaluated as a function of the fatty acid chain length. For the lower homologues of the series columnar liquid-crystalline stacking structures were found, whereas for the higher homologues, lamellar phases predominated. A model for the columnar stacking arrangement, consisting of a unique arrangement of the molecules which could lead to the creation of multiple internal ion channels between the hydrophobic interior and the hydrophilic exterior of the columns, is suggested.

Keywords: liquid crystals · self-assembly · sucrose · surfactants

Introduction

Sucrose fatty acid esters are often used in the food and cosmetics industries, where their excellent physical properties in terms of emulsification, mildness and toxicology make them ideal candidates as non-ionic surfactants.[1–12] Due to their structural complexity (mixtures with different substitution degrees and regioisomers), the physico-chemical properties of defined sucrose compounds have been less extensively studied compared with other types of non-ionic surfactants, for example polyoxyethylenic surfactants or alkylpolyglucosides. Although surface and related properties of monosubstituted sucrose esters in solution are well-documented,[13–22] their thermotropic liquid crystal properties have not been investigated in detail to date, except for a study of a defined mixture of sucrose oleate.[23] More recently, shear induced phase transitions of sucrose stearate blends have also been investigated.[21]

Most amphiphiles, which contain sugars or cyclic and acyclic polyols as polar heads, have been found to exhibit smectic A* phases.[24–26] A limited number of inverted thermotropic, disordered columnar mesophases have also been obtained by grafting several fatty chains on to the polar head group, thus increasing the volume ratio of fatty chain to polar head group, thereby leading to changes in curvature.[27,28] Inverted hexagonal columnar mesophases have been obtained by increasing the volume of the head group from a single-sugar head to double-sugar head, but still with the attachment of a single aliphatic chain. Interestingly, in

[a] Dr. V. Molinier, Dr. J. Fitremann, Dr. A. Bouchu, Dr. Y. Queneau
Laboratoire de Chimie Organique, UMR 5181 CNRS-UCBL-INSA
Institut National des Sciences Appliquées de Lyon
Bât. J. Verne, 20 avenue A. Einstein
69621 Villeurbanne Cedex (France)
Fax: (+33) 4724-38896
E-mail: yves.queneau@insa-lyon.fr

[b] Prof. J. W. Goodby
Department of Chemistry, The University of York
Heslington, York, YO10 5DD (UK)
Fax: (+44) 1904-432-516
E-mail: jwg500@york.ac.uk

[c] Dr. P. J. J. Kouwer, Dr. G. Mackenzie
Department of Chemistry, The University of Hull
Cottingham Road, Hull, HU6 7RX (UK)

[d] Dr. V. Molinier
Current address:
Laboratoire de Chimie Organique et Macromoléculaire
UMR CNRS 8009, École Nationale Supérieure de Chimie de Lille
BP 108, 59652 Villeneuve D'Ascq Cedex (France)

[e] Dr. P. J. J. Kouwer
Department of Chemistry, MIT
77 Massachusetts Avenue
Cambridge MA 02139-4307 (USA)

[f] Dr. J. Fitremann
Laboratoire des IMRCP, CNRS UMR 5623
Université Paul Sabatier, Bât. II R 1
118 Route de Narbonne
31062 Toulouse Cedex 4 (France)

such molecular architectures which maintain a rod-like shape, as it is the case for most alkylpolyglucosides, smectic A* phases are again observed.[29–31] However, when the polar head is not only more bulky, but also takes a wedge-shaped conformation, as in the case of certain regioisomers of sucrose hydroxyalkylethers, columnar or cubic mesophases are observed.[32,33]

In order to gain insight into the self-organizing, thermotropic and lyotropic behaviours of glycolipids, and eventually connect these properties to those of associated compounds found in biological systems,[34–37] we describe the thermotropic behaviour of pure monosubstituted sucrose esters of defined structure, namely the compound families **1** to **3**, as a function of chain length (*n*) and the position of attachment to the sucrose scaffold (i.e., the 1′, 6 and 6′-substituted systems), as shown below. In addition, unsaturated fatty chains, possessing a double bond with a *cis* geometry, as often found in nature, were also included in the investigation.

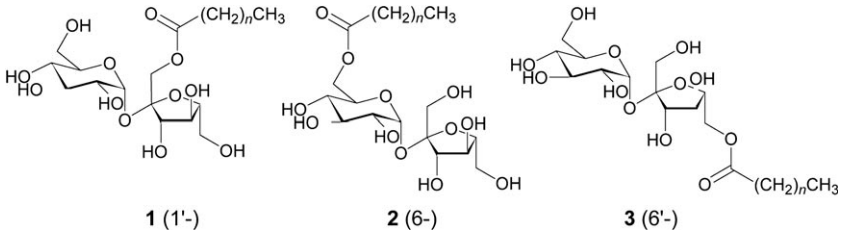

Experimental Section

General synthetic methods: Compounds **1a–f**, **2a–h** and **3a–e**, with chain lengths and levels of unsaturation as shown in Tables 1 and 4, were synthesised from unprotected sucrose, using selective methods of esterification.[38] The 1′-monoesters, **1a–f**, were prepared by enzymatic methods, see Scheme 1, whereas the 6-monoesters, **2a–h**, and the 6′-monoesters, **3a–e**, were obtained by Mitsunobu coupling reactions, see Scheme 2.[39] These methods, though very selective, did not yield totally pure regioisomers, therefore further purification was performed by preparative HPLC. Due to migration phenomena,[40,41] other regioisomers could not be synthesised in the pure form.

Enzymatic synthesis of sucrose monoesters 1a–f: The 1′-monoesters, **1a–f**, were obtained by transesterification of unprotected sucrose with the corresponding vinylic ester in hydrated dimethyl formamide, and in the presence of a selected protease.[42–45] The isolated monoesters contained from 67 to 76% of the 1′-isomer together with the 6 and 6′-isomers. Compounds **1c–f** were further purified by semipreparative HPLC to give the pure 1′-*O*-isomer. Materials **1a** and **1b**, for which purification proved to be very difficult, were used as mixtures (**1a** contained 75% of the 1′-isomer, 7% of the 6-isomer and 12% of the 6′-isomer, and for compound **1b**, 76% of the 1′-isomer, 11% of the 6-isomer and 10% of the 6′-isomer).

Synthesis of sucrose monoesters 2a–h and 3a, 3c–e by the Mitsunobu reaction: The 6-monoesters **2a–h** and the 6′-monoesters **3a**, **c–e** were obtained by the reaction of sucrose with the appropriate carboxylic acid under the Mitsunobu conditions.[36,37,39] The isolated monoester fraction, which typically contained approximately 85% of the 6-isomer and 15% of the 6′-isomer, was subjected to purification using semi-preparative HPLC to give the pure 6- isomers and 6′- isomers.

In order to limit the content of water in the products, all of the sucrose monoesters were freeze-dried. The purities of the compounds were determined by ^{1}H and ^{13}C NMR, HPLC, HRMS and elemental analysis (when enough sample was available).

Detailed syntheses of the sucrose monoesters: Compounds **1a**,[45] **1b**,[45] **1c**,[45,46] **1e**,[46] **2a**,[40,47] **2c**,[45,47,48] **2d**,[48] **2e**,[47,48] **3c**,[42] were prepared according to the literature. The spectroscopic data obtained was the same as that reported, whereas compounds **2b**, **f**, **g**, **h**, **3d**, and **e** were prepared according to the methods reported by Molinier et al.[39] The syntheses of the remaining materials,

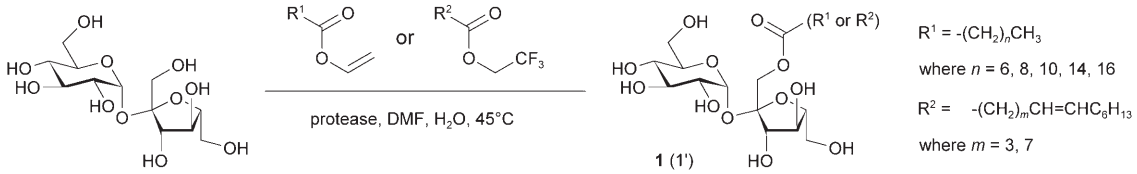

Scheme 1. Synthesis of the saturated and unsaturated sucrose 1′-monoesters, series **1**, by enzymatic methods.

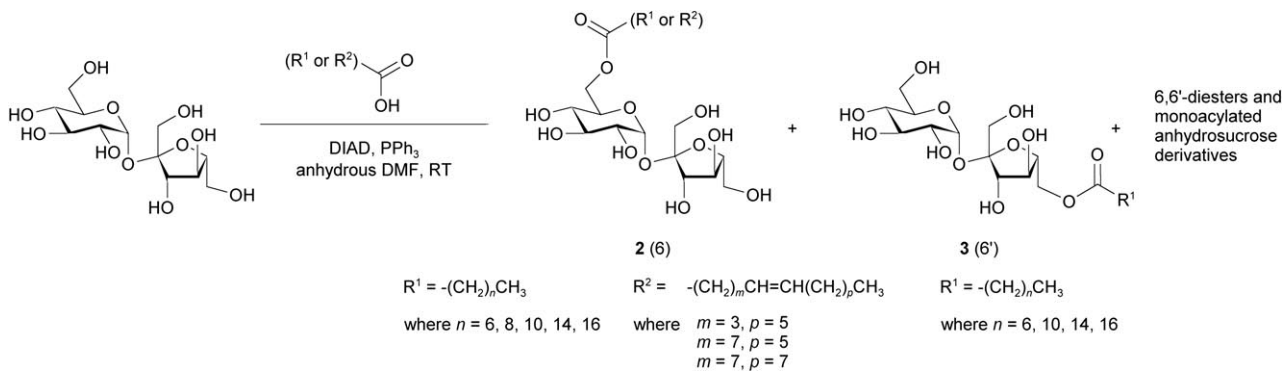

Scheme 2. Synthesis of the 6- and 6′-sucrose monoesters (series **2** and **3**) via the Mitsunobu reaction.

which have not yet been reported in the literature, are described in more detail in the following section.

Synthesis of compounds 1a–f by enzymatic methods: Sucrose, obtained from Béghin-Say, (1.11 g, 3 mmol) was dissolved in a DMF/water mixture 96:4 (8 mL), at a temperature of 45 °C with stirring. The acylating agent, lauric acid vinyl ester (3.65 g, 5 equiv), and protease (Novozyme FM/Celite, 2.5 g, obtained as a gift from Novozyme), were added to the mixture. The temperature of the reaction was maintained at 45 °C for 4 d with slow stirring. After filtration and removal of the DMF by evaporation, the monoester was isolated by flash chromatography (elution of dichloromethane/acetone/methanol/water 56:20:20:4, $R_f = 0.56$ for sucrose monolaurate) and freeze-dried. The monoester was formed with yields ranging from 7 to 61 %, the lower yields were obtained for the products with the longer aliphatic chains. For example, the yield for sucrose monolaurate was 49 %. This material was subjected to purification by semi-preparative HPLC using a NH_2 spherisorb column and an eluent acetonitrile/water[40] in order to isolate pure mono-1′-*O*-ester (67 % to 74 % yield of the monoester fraction).

1′-*O*-Palmitoylsucrose (1d): $[\alpha]_D = +47$ (c = 0.3 in MeOH); ^{1}H NMR (300 MHz, MeOD): δ = 0.80–1.00 (m, 3H, CH_3), 1.15–1.45 (m, 24H, $(CH_2)_{12}$), 1.55–1.73 (m, 2H, $CH_{2\beta}$), 2.39 (t, 2H, $J(CH_2,CH_2) = 7.3$ Hz, $CH_{2\alpha}$), 3.37 (dd, 1H, $J(H_4,H_3) = 9.1$, $J(H_4,H_5) = 9.9$ Hz, H_4), 3.42 (dd, 1H, $J(H_2,H_1) = 3.8$, $J(H_2,H_3) = 9.9$ Hz, H_2), 3.60–3.90 (m, 7H, H_5, $H_{6a/b}$, $H_{6'a/b}$, $H_{5'}$, H_3), 4.00–4.11 (m, 2H, $H_{3'}$, $H_{4'}$), 4.14 (d, 1H, $J(H_{1'b},H_{1'a}) = 12.1$ Hz, $H_{1'b}$), 4.38 (d, 1H, $J(H_{1'a},H_{1'b}) = 12.1$ Hz, $H_{1'a}$), 5.41 (d, 1H, $J(H_1,H_2) = 3.8$ Hz, H_1); LSIMS: m/z: calcd for $C_{28}H_{52}O_{12}Li$: 587.3619; found: 587.3645 $[M]^+$.

1′-*O*-Dodec-5*c*-enoylsucrose (1f): $[\alpha]_D = +44$ (c = 0.7 in MeOH); ^{1}H NMR (500 MHz, MeOD): δ = 0.87–0.99 (m, 3H, CH_3), 1.24–1.43 (m, 8H, $(CH_2)_4$), 1.70 (q, 2H, $J(CH_2,CH_2) = 7.5$ Hz $CH_{2\beta}$), 2.01–2.16 (m, 4H, $CH_2CH{=}CHCH_2$), 2.40 (t, 2H, $J(CH_2,CH_2) = 7.5$ Hz, $CH_{2\alpha}$), 3.38 (t, 1H, $J(H_4,H_3) = J(H_4,H_5) = 9.5$ Hz, H_4), 3.43 (dd, 1H, $J(H_2,H_1) = 3.9$, $J(H_2,H_3) = 9.9$ Hz, H_2), 3.60–3.88 (m, 7H, H_5, $H_{6a/b}$, $H_{6'a/b}$, $H_{5'}$, H_3), 4.03–4.12 (m, 2H, $H_{3'}$, $H_{4'}$), 4.15 (d, 1H, $J(H_{1'b},H_{1'a}) = 12.2$ Hz, $H_{1'b}$), 4.38 (d, 1H, $J(H_{1'a},H_{1'b}) = 12.2$ Hz, $H_{1'a}$), 5.31–5.49 (m, 3H, H_1, CH=CH); ^{13}C NMR (125 MHz, MeOD): δ = 14.7 (CH_3), 26.3 ($CH_{2\beta}$), 27.8–28.5 ($2\,CH_{2\alpha}$ CH=CH), 24.0, 30.4, 31.1, 33.2 ($4\,CH_2$), 34.7 ($CH_{2\alpha}$), 62.5 (C_6), 63.5 ($C_{6'}$), 64.1 ($C_{1'}$), 71.7 (C_4), 73.3 (C_2), 74.7 (C_5), 74.9 (C_3), 75.2 ($C_{4'}$), 79.1 ($C_{3'}$), 84.1 ($C_{5'}$), 94.4 (C_1), 104.3 ($C_{2'}$), 129.9–132.4 (CH=CH), 174.9 (C=O on 1′); LSIMS: m/z: calcd for $C_{24}H_{42}O_{12}Na$: 545.2574; found: 545.2576 $[M{+}Na]^+$.

Synthesis of the sucrose monoesters 2a–h and 3a, c–e via the Mitsunobu reaction: Sucrose (3.42 g, 10.0 mmol) was dissolved in dry DMF (79 mL) at 70 °C with stirring under a nitrogen atmosphere. The mixture was cooled to room temperature before the addition of triphenylphosphine (7.06 g, 2.7 equiv), the appropriate carboxylic acid (for example, lauric acid, 5.00 g, 2.5 equiv), and more DMF (21 mL). Once the materials had dissolved, the mixture was cooled to 0 °C, and DIAD (5.3 mL, 2.7 equiv) was added. TLC showed the nearly total consumption of sucrose after 26 h stirring at room temperature. After removal of DMF under reduced pressure at T = 36–38 °C, the crude residue was subjected to chromatography over silica gel (dichloromethane/acetone/methanol/water 78:10:10:1.5→67:15:15:3). The monoester fraction was collected (e.g., for monolauroylsucrose, 1.86 g, 35 %) and subjected to further purification by semi-preparative HPLC (NH_2 spherisorb column, acetonitrile/water[40]) in order to isolate the pure mono-6-*O*-ester (e.g. 85 % of the monoester fraction for the monolauroylsucrose) and pure mono-6′-*O*-ester (15 % of the monoester fraction).

6′-*O*-Octanoylsucrose (3a): $[\alpha]_D = +52$ (c = 1 in MeOH); ^{1}H NMR (300 MHz, MeOD): δ = 0.80–1.00 (m, 3H, CH_3), 1.20–1.45 (m, 8H, $(CH_2)_4$), 1.53–1.73 (m, 2H, $CH_{2\beta}$), 2.36 (t, 2H, $J(CH_2,CH_2) = 7.4$ Hz, $CH_{2\alpha}$), 3.35 (t, 1H, $J(H_4,H_3) = J(H_4,H_5) = 9.4$ Hz, H_4), 3.42 (dd, 1H, $J(H_2,H_3) = 9.7$, $J(H_2,H_1) = 3.8$ Hz, H_2), 3.57–3.77 (m, 4H, H_{6b}, H_3, $H_{1'a/b}$), 3.78–3.88 (m, 2H, H_{6a}, H_5), 3.93 (td, 1H, $J(H_{5'},H_{4'}) = J(H_{5'},H_{6'a}) = 7.5$ Hz, $J(H_{5'},H_{6'b}) = 3.3$ Hz, $H_{5'}$), 4.02 (t, 1H, $J(H_{4'},H_{5'}) = J(H_{4'},H_{3'}) = 8.1$ Hz, $H_{4'}$), 4.11 (d, 1H, $J(H_{3'},H_{4'}) = 8.1$ Hz, $H_{3'}$), 4.32 (dd, 1H, $J(H_{6'b},H_{6'a}) = 11.7$, $J(H_{6'b,5'}) = 3.3$ Hz, $H_{6'b}$), 4.41 (dd, 1H, $J(H_{6'a},H_{6'b}) = 11.7$, $J(H_{6'a},H_{5'}) = 7.5$ Hz, $H_{6'a}$), 5.36 (d, 1H, $J(H_1,H_2) = 3.8$ Hz, H_1); ^{13}C NMR (75 MHz, MeOD): δ = 14.7 (CH_3), 26.3 ($CH_{2\beta}$), 24.0, 30.4, 30.4, 33.2 ($4\,CH_2$), 35.2 ($CH_{2\alpha}$), 62.8 (C_6), 64.1 ($C_{1'}$), 67.2 ($C_{6'}$), 71.8 (C_4), 73.6 (C_2), 74.5 (C_5), 75.0 (C_3), 77.2 ($C_{4'}$), 79.2 ($C_{3'}$), 81.0 ($C_{5'}$), 93.7 (C_1), 105.8 ($C_{2'}$), 175.8 (C=O on 6′).

Evaluation of physical properties: Phase identification and the determination of phase transition temperatures were carried out by thermal polarised light microscopy (POM), by using a Zeiss Universal polarising transmitted light microscope equipped with a Mettler FP82 microfurnace in conjunction with an FP50 Central Processor. Photomicrographs were obtained using a Zeiss polarising light microscope equipped with a Nikon AFM camera. Homogeneous specimens were obtained by using untreated glass slides and cover slips. Differential scanning calorimetry was used to determine enthalpies of transition and to confirm the phase transition temperatures determined by optical microscopy. Differential scanning thermograms (scan rate 10 °C min^{-1}) were obtained by using a Perkin–Elmer DSC7 PC system operating on DOS software. The results obtained were standardised to indium (measured onset 156.68 °C, ΔH = 28.47 J g^{-1}; lit. value 156.60 °C, ΔH = 28.45 J g^{-1}).[49] Comparison of the transition temperatures determined by optical microscopy and differential scanning calorimetry show some slight discrepancies, which are due to the carbohydrate moieties which tended to decompose at elevated temperatures and at different rates depending on the rate of heating, the time spent at an elevated temperature and the nature of the supporting substrate, that is, the materials decomposed more quickly in aluminium DSC pans than on glass microscope slides.

The X-ray diffraction experiments were performed using a MAR345 diffractometer equipped with a 2D image plate detector ($Cu_{K\alpha}$ radiation, graphite monochromator, $\lambda = 1.54$ Å). The samples were heated in the presence of a magnetic field ($B \approx 1$ T) by using a home-built capillary furnace. The diffraction patterns show the intensity as a function of the modulus of the scattering wave vector (q) as in Equation (1).

$$q = |q|\,4\pi\sin\theta/\lambda = 2\pi n/d \quad (1)$$

where θ is the diffraction angle, λ is the wavelength (1.54 Å), n is an integer and d is the lattice distance.

Molecular lengths were determined either by using Dreiding molecular models or via computer simulations using an Apple MacIntosh G5 computer and ChemDraw3D as part of a ChemDraw Ultra 6.0 program.

Results and Discussion

The materials were segregated into two groups by the nature of the aliphatic chains. Thus the first group to be discussed has saturated fatty chains, that is monoesters **1a–e**, **2a–e** and **3a**, **3c–e**; the second group has analogues possessing a *cis*-unsaturated double bond in the middle of the chain, that is **1f**, **2f**, **2g** and **2h**.

Saturated fatty acid monoesters

Transition temperatures: The mono-1′- (series **1**), mono-6- (series **2**) and mono-6′- (series **3**) esters of sucrose were examined in their dry state by thermal polarised light microscopy (POM) and differential scanning calorimetry (DSC). While the clearing points from the liquid crystalline state to the isotropic liquid were clearly discernable by POM, decomposition caused by caramelisation meant for many of the materials that, although the clearing points could be determined by DSC, the associated enthalpy values could not be measured. Decomposition caused the baseline of the heating thermogram to fluctuate strongly after the clearing

point transition, suggesting that the materials were more stable in the liquid-crystal state than in the amorphous liquid. In most cases the melting points could not be determined by POM due to either paramorphosis of the defect textures at the phase transition or if the transition was from a glassy solid to the mesomorphic state no discernable change in texture could be detected. Thus, Table 1 summarises the most clearly defined results obtained concerning melting behaviour of the compounds possessing saturated aliphatic chains.

The first members of the three series, that is the shortest aliphatic homologues **1a**, **2a** and **3a**, in all cases were found to exhibit disordered hexagonal columnar phases. Figure 1 shows a photomicrograph of the defect texture of mono-6′-*O*-octanoylsucrose (**3a**). This texture is typical of the first members of each of the series. Under crossed polarizers (×100), fan-like defects of the liquid crystal phase were observed, and in some cases a homeotropic uniaxial defect texture was also observed. In the fan-like texture, no hyperbolic or elliptical lines of optical discontinuity associated with focal-conic defects were observed, indicating that the phase is probably not a lamellar/smectic phase.[50] The fan-like regions indicate that the phase is columnar, and the lack of ordering (straight-lines) along the column edges suggests that the mesophase is disordered. These results were confirmed by X-ray diffraction (see later).

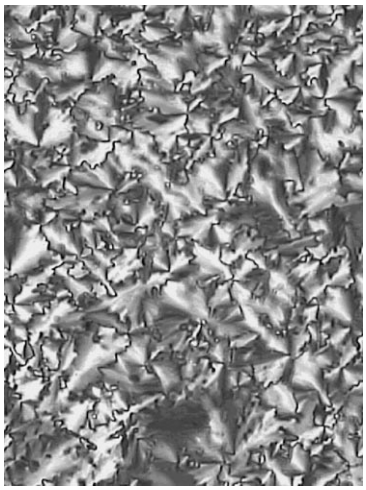

Figure 1. Defect texture of the columnar mesophase of mono-6′-*O*-octanoylsucrose (**3a**) (×100).

The mono-6-*O*-decanoyl sucrose (**2b**) was also found to exhibit a fan-like defect texture in which no hyperbolic or elliptical lines of optical discontinuity were observed (see Figure 2). For this reason, the mesophase formed by this compound was initially classified as a columnar phase, however, structural studies show that it is probably a smectic A* phase (see X-ray results later).

All of the other sucrose monoesters exhibited typical textures for the smectic A* phase (see Figure 3). We note that the classification of the mesophase is smectic A*, because as the materials are chiral the environmental symmetry of the phase is reduced from $D_{8\infty}$ to D_{∞}, and as a consequence the mesophase should exhibit electroclinic properties. In order to determine the type of mesophase formed by the longest chain analogues and to limit the degradation of the products (caramelisation), the samples were brought quickly to a temperature above their clearing point and cooled down to observe the texture.

Under crossed polarisers, a homeotropic black texture was observed, together with a fan-like defect texture possessing elliptical and hyperbolic lines of optical discontinuity. Oily streaks and fringes around air bubbles were also observed. Upon cooling from the isotrop-

Table 1. Transition temperatures of the mono-1′ (series **1**), mono-6 (series **2**) and mono-6′ (series **3**) saturated fatty acid sucrose esters.[a]

Sucrose monoesters	Chain	Compd	Transition temperatures [°C]
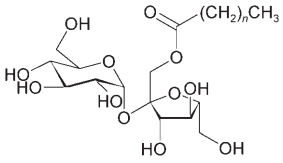	$n=6$	**1a**$^{(*)}$	soft solid–columnar 90 Iso Liq
	$n=8$	**1b**$^{(*)}$	soft solid–SmA* 145 iso liq
	$n=10$	**1c**	glass 46.2 SmA* 186.8 iso liq
	$n=14$	**1d**	cryst 53.8 SmA* 209.5 iso liq
	$n=16$	**1e**	cryst 48.5 SmA* 210 iso liq
1′-*O*-esters (series **1**)			
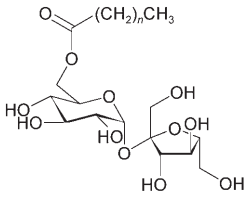	$n=6$	**2a**	soft solid–columnar 95.6 iso liq
	$n=8$	**2b**	soft solid–SmA* 107 iso liq
	$n=10$	**2c**	cryst 65.8 SmA* 179.5 iso liq
	$n=14$	**2d**	cryst 72.4 SmA* 212 iso liq
	$n=16$	**2e**	cryst 39.3 SmA* 212 iso liq
6-*O*-esters (series **2**)			
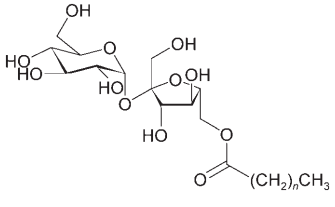	$n=6$	**3a**	soft solid–columnar 105 iso liq
	$n=10$	**3c**	crystal SmA* 204.5 iso liq
	$n=14$	**3d**	crystal SmA* 225.5 iso liq
	$n=16$	**3e**	crystal SmA* 211 iso liq
6′-*O*-esters (series **3**)			

[a] Soft solid refers to transitions not seen in the DSC, whereas cryst refers to melting points determined by DSC. $^{(*)}$ mixtures of isomers: **1a**: 6/1′/6′ 7:75:12%, **1b**: 6/1′/6′ 11:76:10%.

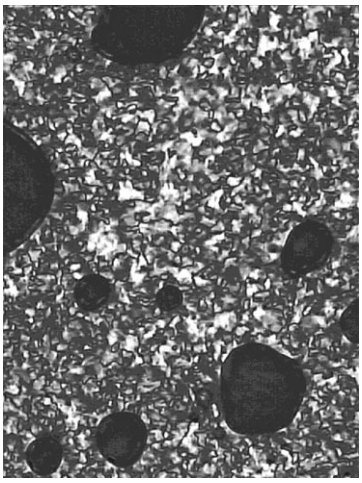

Figure 2. Defect texture of the mesophase exhibited by mono-6-*O*-decanoylsucrose (**2b**) (×100).

ic liquid, the liquid crystal phase separated in the form of *bâtonnets* that coalesced to form the focal-conic domains. These features are characteristic of smectic A/A* mesophases. They are highlighted with white arrows in the textures shown in Figure 3.

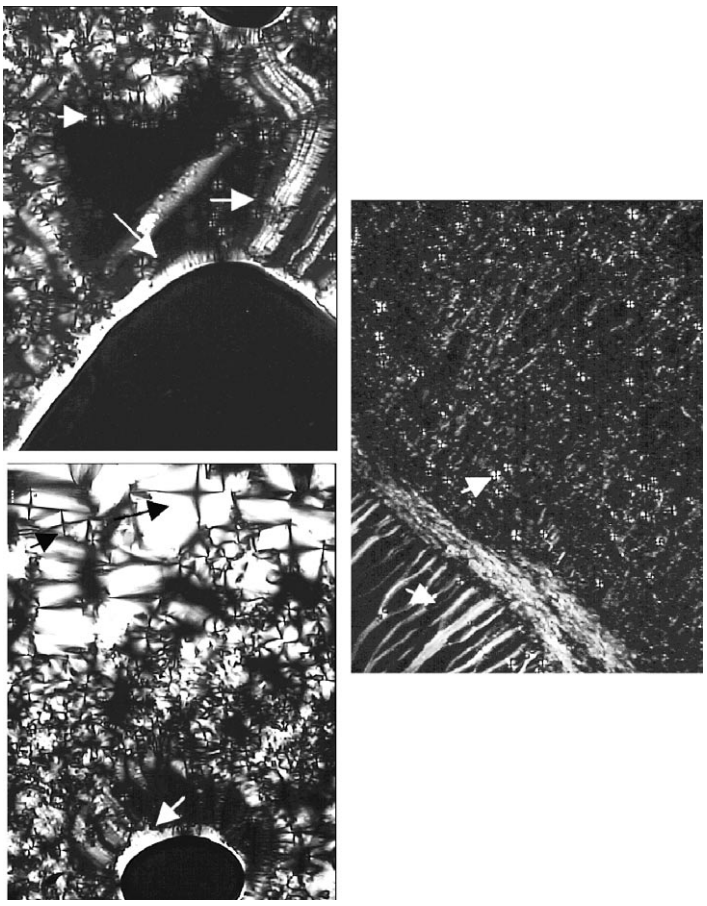

Figure 3. Defect textures of smectic A* mesophases of mono-dodecanoylsucrose (**2c**, top and bottom) and mono-6-*O*-hexadecanoylsucrose (**2d**, right).

The evolution of the isotropisation temperature (clearing point) as a function of the length of the fatty chains is shown in Figure 4. The values plotted were the ones determined for the first heating cycle, at a point when all of the birefringence disappeared. For compounds **1c–e**, **2c–e** and **3c–e**, the transition to the isotropic liquid took place at the point where caramelisation started to occur, and as noted above, caramelisation appeared to be accelerated at the phase transition to the liquid.

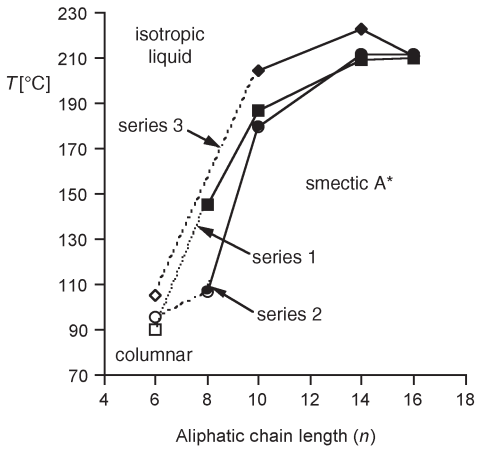

Figure 4. Evolution of the clearing point [°C] as a function of the length of the fatty aliphatic chains (*n*) for the sucrose monoesters **1a–e** (■), **2a–e** (●) and **3a**, and **3c–e** (◆).

It can be seen from Figure 4 that the columnar phases are less thermally stable in comparison to the lamellar phases. In some cases the lamellar phase occurs at temperatures approximately 100 °C higher than the corresponding columnar phase. Columnar phases are only found for the homologues with short chains, and the maximum stability of the lamellar phase occurs at approximately the hexadecanoyl (C_{16}) homologue.

Differential scanning calorimetry: For sucrose monoesters, differential scanning calorimetry often showed the effects of decomposition before the isotropic liquid was reached. The decomposition was believed to be due to the high clearing point values, and that the rate of decomposition was more rapid when the materials were evaluated in aluminium pans, rather than when observed between the glass slide and cover-slip in POM.

For the materials with the shorter chains, each material appears to be in its mesomorphic state at or near to room temperature, since no melting peak is observed on the DSC and only glass transitions were obtained. Conversely, the longer chain analogues often undergo complex melting from the solid to the liquid crystal state, with many solid–solid transitions occurring. Upon cooling, these materials undergo either a partial recrystallisation, or no recrystallisation at all, with the liquid crystalline state remaining down to room temperature. In some cases a glass transition close to room

temperature can be discerned. Thus for the longer chain length materials the liquid crystal state can remain in a metastable form over wide temperature ranges.

By way of example, the DSC thermogram for mono-1′-*O*-dodecanoylsucrose (**1c**) is presented in Figure 5. For this compound, the melting from the solid to the liquid crystal proceeds via a glass transition, however, the transition to the isotropic liquid is clearly defined. In contrast, Figure 6 shows the DSC thermogram for the first heating and cooling cycles of mono-6-*O*-octadecanoylsucrose (**2e**). For this compound, degradation is observed at the clearing point. The fluctuations in the baseline reflect the process of caramelisation. Upon cooling from the isotropic liquid no enthalpy is observed at a temperature where the clearing point occurred, and indeed no phase transition was detected until the point at where the material recrystallised.

This type of inconsistent behaviour thus made it difficult to obtain data for each material that could be used for comparative purposes within, and between, the series of compounds. Moreover, because of the ease of decomposition, even where results seemed to be conclusive, it was difficult to exclude the possibility of degradation.

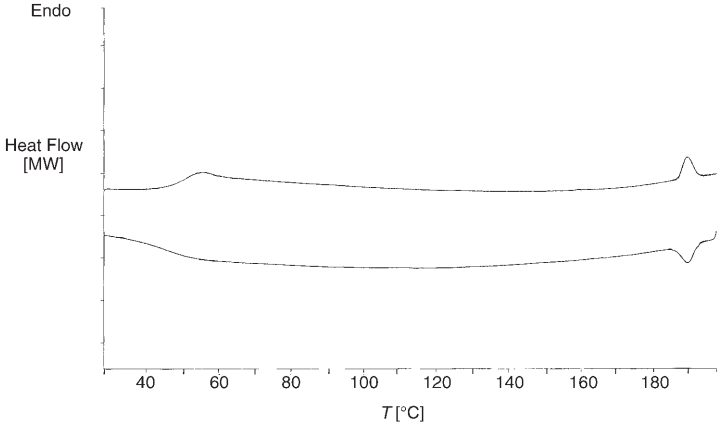

Figure 5. DSC thermogram, first heat and first cool cycles, for mono-1′-*O*-dodecanoylsucrose (**1c**) at a scanning rate 10 °C min^{-1}.

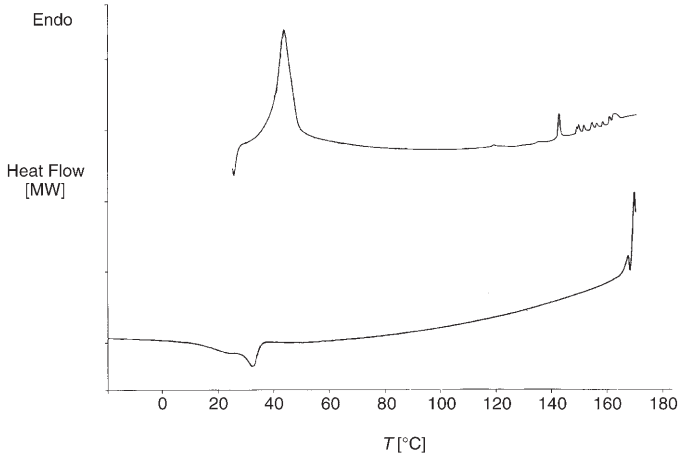

Figure 6. DSC trace, first heating and cooling cycles, for mono-6-*O*-octadecanoylsucrose (**2e**) at a scanning rate 10 °C min^{-1}.

X-ray diffraction studies: For the purposes of comparison and the evaluation of the structures of materials with columnar and lamellar phases X-ray diffraction studies were performed on compounds **2a**, **2b** and **2e** over a wide range of temperature in the mesomorphic state.

X-ray diffraction studies of mono-6-O-octanoylsucrose (2a): Figure 7 shows the diffraction pattern of compound **2a** at 80 °C. The radially integrated pattern at 30 °C is shown in Figure 8; Table 2 gives the relative distances in Å relative to the Miller indices.

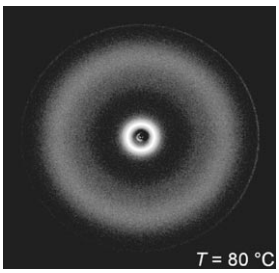

Figure 7. Powder diffraction pattern of mono-6-*O*-octanoylsucrose (**2a**) at 80 °C.

The first three distances are in the ratios 1, $1/\sqrt{3}$, $1/\sqrt{4}$, which are characteristic of a hexagonal packing arrangement of the molecules. X-ray diffraction studies thus confirm the microscopic observations and give the classification of the mesomorphic phase of mono-6-*O*-octanoylsucrose (**2a**) as a hexagonal columnar phase. The diffuse reflection at 4.5 Å

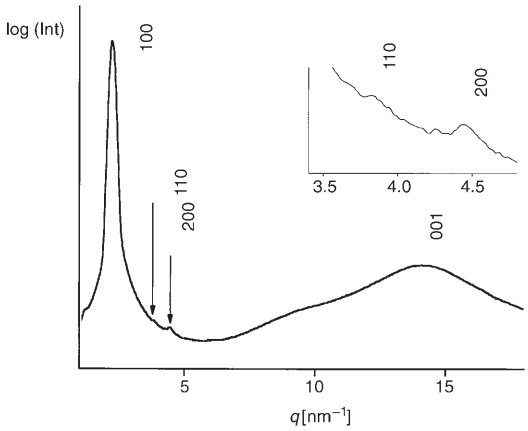

Figure 8. Radially integrated diffraction pattern of mono-6-*O*-octanoylsucrose (**2a**) at 30 °C. The diffraction intensity is given in a logarithmic scale.

Table 2. Distances related to the Miller indices shown in the diffraction pattern given in Figure 8 for the radially integrated diffraction pattern of mono-6-*O*-octanoylsucrose (**2a**) at 30 °C.

Miller Indices	q [nm^{-1}]	d [Å]	Ratios
100	2.24	28.1	1
110	3.85	16.3[a]	$0.580 \approx 1/\sqrt{3}$
200	4.49	14.0	$0.498 \approx 1/\sqrt{4}$
001	9.5	6.6	–
alkyl	14.1	4.5	–

[a] Very weak reflection.

shows that the ordering of the aliphatic chains inside the column is low, indicating that the phase is a disordered hexagonal phase. Furthermore, the reflection observed at 6.6 Å could be attributed to extensive ordering of the sugar head groups.

X-ray diffraction studies of mono-6-O-decanoylsucrose (2b): Figure 9 shows the radially integrated patterns for compound **2b** at various temperatures. No second order reflections were observed for this material, thereby indicating the presence of a smectic mesophase. Conversely, the microscopic observations suggested the formation of a columnar mesophase.

For mono-6-*O*-decanoylsucrose (**2b**) no changes were observed at the clearing point observed by optical microscopy, that is, $T_i = 107\,°C$. Figure 10 shows the normalised, azimuthally integrated patterns at 85 and 140 °C, which demonstrates that at high temperatures substantial ordering of the molecules is maintained, despite degradation of the sample. Thus, remarkably the "amorphous liquid" appears to be structured at temperatures well away from the liquid crystalline state.

X-ray diffraction studies of mono-6-O-octadecanoylsucrose (2e): X-ray diffraction studies were performed over a 30 to 160 °C temperature range for the mono-6-*O*-octadecanoylsucrose (**2e**), see Figure 11. The radially integrated patterns at 140 and 30 °C are shown together in Figure 12 and Table 3 gives the distances in Å related to the Miller indices at $T =$ 30, 50 and 130 °C, respectively.

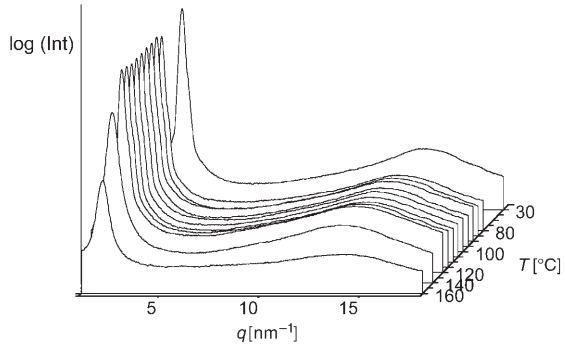

Figure 9. Radially integrated diffraction pattern of mono-6-*O*-decanoylsucrose (**2b**) over a 30 to 100 °C temperature range. The diffraction intensities are given in a logarithmic scale.

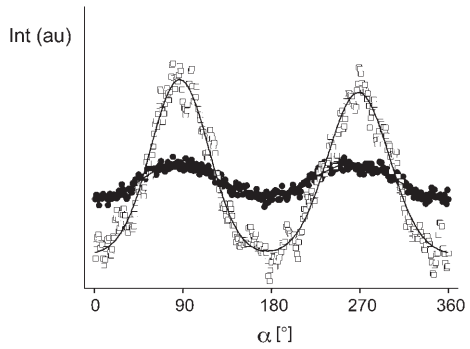

Figure 10. Normalised azimuthally integrated patterns of 6-*O*-monodecanoylsucrose (**2b**), □: $T = 85\,°C$, ●: $T = 140\,°C$.

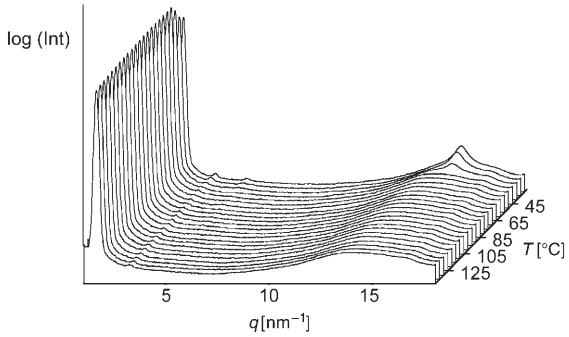

Figure 11. Radially integrated diffraction pattern of mono-6-*O*-octadecanoylsucrose (**2e**) over a 30 to 160 °C temperature range. The diffraction intensities are given in a logarithmic scale.

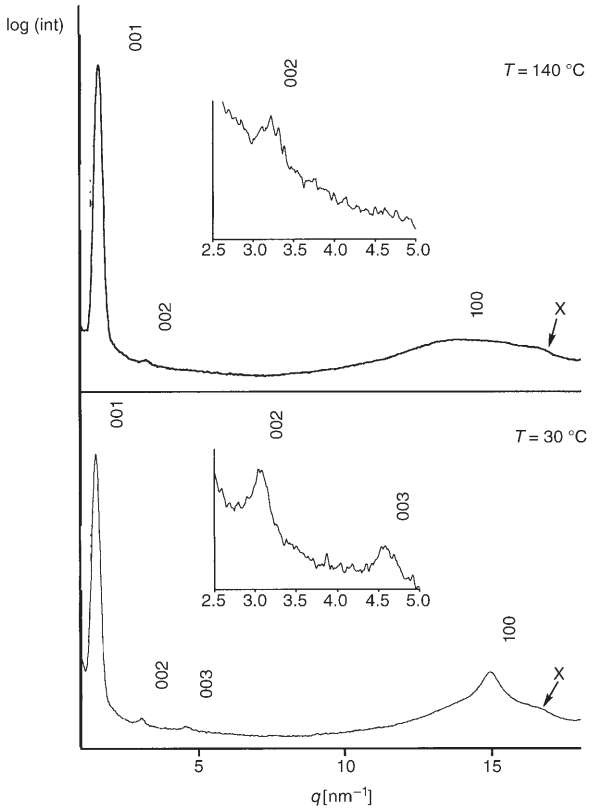

Figure 12. Radially integrated diffraction patterns of mono-6-*O*-octadecanoylsucrose (**2e**) at 140 and 30 °C. The diffraction intensities are given in a logarithmic scale.

With the ratios between the first three *d* spacings being characteristic of a lamellar arrangement, X-ray diffraction studies for the mono-6-*O*-octadecanoylsucrose (**2e**), confirm the microscope classification of the phase as smectic A. However, as the extended length of the material determined

Table 3. Distances related to the Miller indices shown in Figure 11 for the radially integrated diffraction pattern of mono-6-*O*-octadecanoylsucrose (**2e**) at 30, 50 and 130 °C, respectively.

Miller indices	q [nm^{-1}]	d [Å]	Ratios
$T=30$ °C			
001	1.52	41.3	1
002	3.06	20.5	$\approx 1/2$
003	4.58	13.7	$\approx 1/3$
100 + alkyl	14.7	4.3	–
X	16.5	3.8	
$T=50$ °C			
001	1.53	41.2	1
002	3.04	20.7[a]	$\approx 1/2$
100 + alkyl	14.2	4.4	–
X	16.5	3.8	–
$T=130$ °C			
001	1.61	39.1	1
002	3.18	19.8[a]	$\approx 1/2$
100 + alkyl	14.7	4.55	–
X	16.5	3.8	–

[a] Very weak reflection.

from simulations was found to be approximately 28 Å, and the measured layer spacing being approximately 41 Å, the structure of the phase must consist of interdigitated bilayers. Thus, the phase is further classified as a smectic A_d modification.

The aliphatic chains inside the layers are disordered, as indicated by the diffuse reflection at 4.3 Å. Conversely, the reflection observed at 3.8 Å could be attributed to well-organised arrays of sugar head groups due to H-bonding. The temperature scan shows that at a temperature lower than 40 °C, the smectic phase becomes more strongly ordered as now the third order reflection is observed.

Thus, overall the early members of series **2** possess disordered hexagonal columnar phases, whereas the later members of the series exhibit interdigitated bilayer smectic A_d phases. The amorphous liquid in all of the materials is structured to high temperatures, which is possibly due to hydrogen-bonding networks formed by the interactions of the sucrose head groups. In the mesophases the aliphatic chains are effectively melted, whereas the sugar head groups are extensively organised.

Unsaturated fatty acid monoesters

In order to investigate the effects of the incorporation of a *cis*-double bond into the terminal aliphatic chains compounds **1f** and **2f–h** were prepared. It was expected that the presence of the *cis*-bond would "kink" the aliphatic chain, thereby leading to an increase in disordering of the molecules and a concomitant lowering of the clearing points.

Microscopy studies showed that compounds **1f** and **2f–h**, like their saturated analogues, exhibited smectic A mesophases. Figure 13 shows examples of the edge dislocation (filaments) and homeotropic textures of mono-6-*O*-dodec-5*c*-enoylsucrose (**2f**). These textures are classical examples of a lamellar phase.

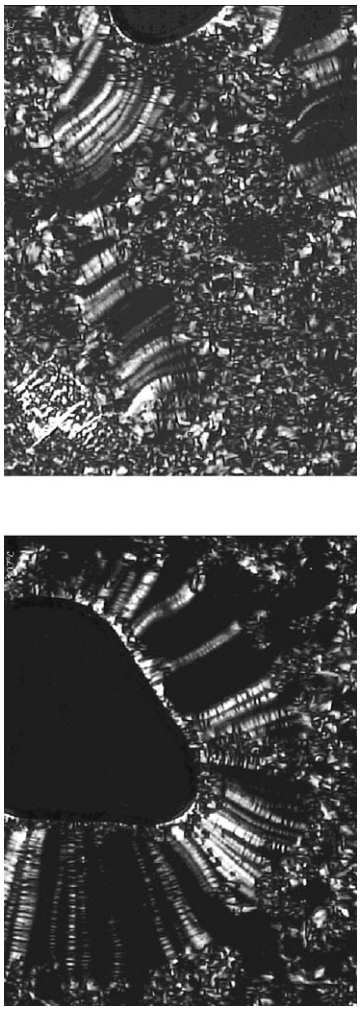

Figure 13. Defect textures of the smectic A* mesophase of mono-6-*O*-dodec-5*c*-enoylsucrose (**2f**) (×100).

Table 4 shows the structures of compounds **1f** and **2f–h**, together with their clearing points and the comparative values for the directly analogous materials with no unsaturations in the aliphatic chain. It can be seen that when the double bond is near to the sucrose head group the clearing point is substantially lower in comparison to the saturated ester. However, when the double bond is further away from the sucrose head group the difference in clearing points is much less. This is possibly due to the fact that the chains will be essentially melted in the smectic state, and when the double bond is nearer to the more rigid structure of the head group, the freedom of the methylene units in the chain to rotate is somewhat restricted.

Modelling of mesophase structures: If we now turn to the question as to why the saturated esters with relatively short aliphatic chains exhibit columnar phases, whereas the higher homologues exhibit lamellar phases, we can explain this result simply through examination of the minimised molecular structures, albeit in the gas phase, of the octanoyl versus the octadecanoyl homologues of any of the three series. For

Table 4. Structures and clearing point transitions for the unsaturated monoesters **1f** and **2f–h**.[a]

Monoesters	Compound	Clearing point transitions
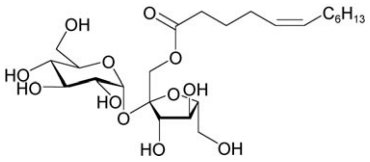	**1f**	Iso Liq 165 °C SmA*
	1c	Iso Liq 186.8 °C SmA*
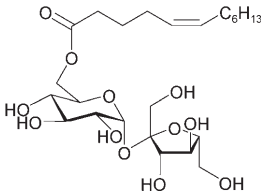	**2f**	Iso Liq 132.8 °C SmA*
	2c	Iso Liq 179.5 °C SmA*
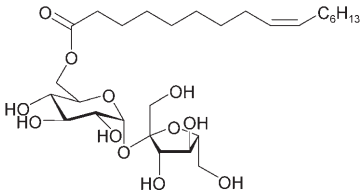	**2g**	Iso Liq 207 °C SmA*
	2d	Iso Liq 212 °C SmA*
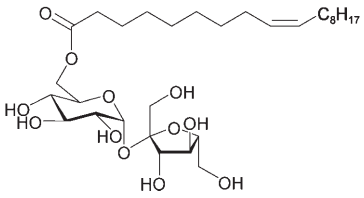	**2h**	Iso Liq 205 °C SmA*
	2e	Iso Liq 212 °C SmA*

[a] The clearing point transitions for the analogous saturated materials **1c** and **2c–e** are included for comparison.

example, if we select series **2**, and therefore compounds **2a** and **2e**, we find that the minimised structures show that the head-group size relative to the overall molecular length is much greater for **2a** than for **2e**. Thus when the molecules of **2a** pack together they will do so with a curved structural arrangement favouring the formation of columnar phases, whereas such an arrangement would be less likely for **2e**, and thereby lamellar phases are preferred. Figure 14 shows the minimised structures for **2a** and **2e** achieved in the gas phase, at absolute zero. Compound **2a** clearly has a more wedge liked structure than **2e**.

Further hypotheses can be derived from the minimised structures. It appears that intramolecular hydrogen bonding between the carbonyl function of the ester and one of the hydroxyl units causes the sucrose head group to bend back on itself, thereby exposing the rest of the hydroxyl groups to the exterior of the structure, away from the aliphatic chain. This is an unusual molecular arrangement in light of the report by Perez et al.,[51] which shows for 2-*O*-lauroylsucrose that an intramolecular hydrogen bond between the 6,6′-OH groups stabilises the cyclic arrangement of the head group. Nevertheless, for the three series, shown in Figure 15, gas-phase modelling shows that the carbonyl-OH hydrogen bond is slightly favoured. Consequently, the intramolecular hydrogen bond apparently completes a quasi-macrocyclic structure, which is sandwiched between the hydrophilic head group and the hydrophobic chain. The quasi-macrocyclic structure appears as a cyclic polyether, and thereby should be capable of complexing various ions. Thus the sucrose esters appear to have a remarkable structure; the head group is forced by an intramolecular hydrogen bond to expose all of its free hydroxyl groups for the purposes of intermolecular hydrogen bonding, and behind this hydrophilic wall a binding site sits, protected on one side by a hydrophilic surface while on the other by a hydrophobic chain as shown in Figure 16.

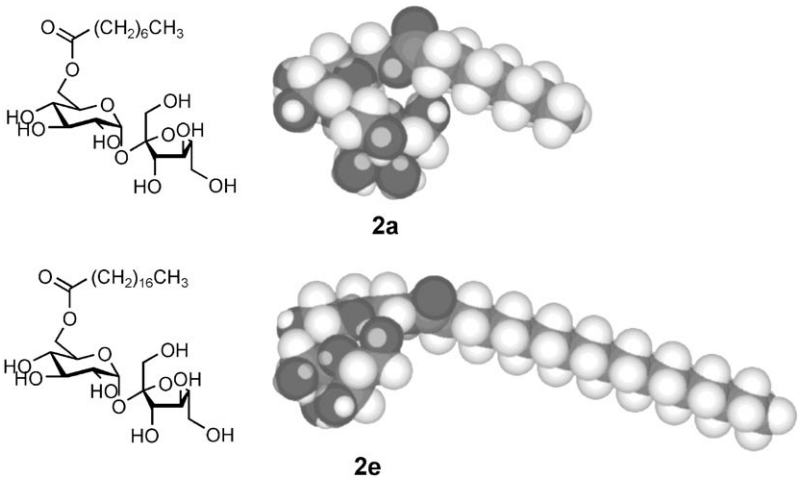

Figure 14. Minimised structures of compounds **2a** and **2e** in the gas phase at absolute zero.

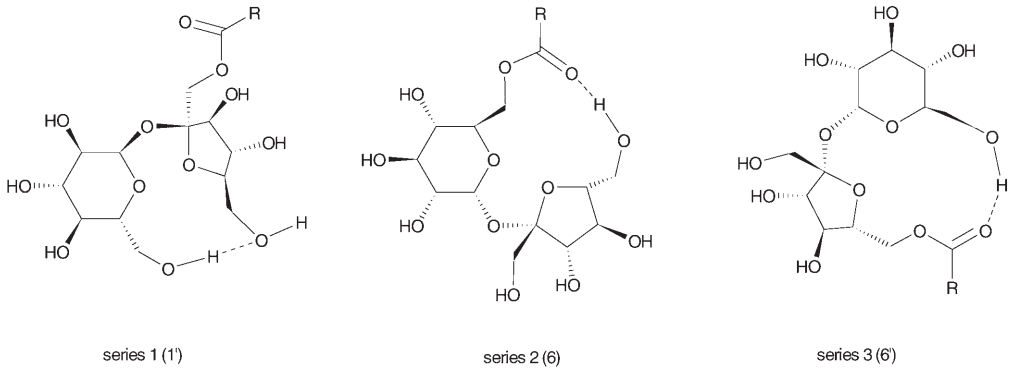

Figure 15. Intramolecular hydrogen bonding in the head groups of all three series, forming a quasi-macrocyclic ring system.

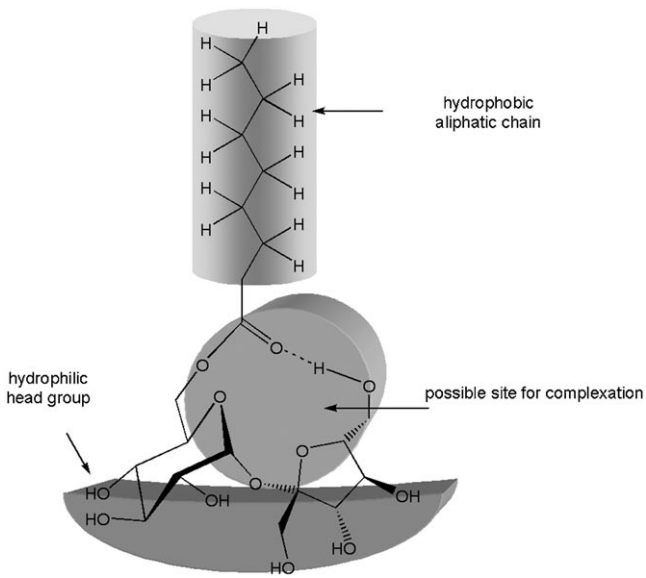

Figure 16. Composite parts of the structure of the mono-substituted sucrose esters.

For the columnar phases, be they thermotropic or lyotropic, the self-organised structure consists of three tubes where the outer tube can interact with solvents such as water or with similarly stacked columns through intermolecular hydrogen bonding. The central tube is filled with hydrophobic fatty material, and the space between the outer and inner tubes is a region where the quasi-macrocycles can also assemble into internal columns, like a roller-bearing race, thereby creating potential ion channels, as shown in Figure 17.

Conclusion

In this report we show that for sucrose substituted with one aliphatic chain in the 1′, 6 or 6′ positions, for relatively short aliphatic chains columnar liquid crystals phases are favoured over calamitic lamellar phases. The structure of the columnar phase is suggested to be one where the aliphatic chains

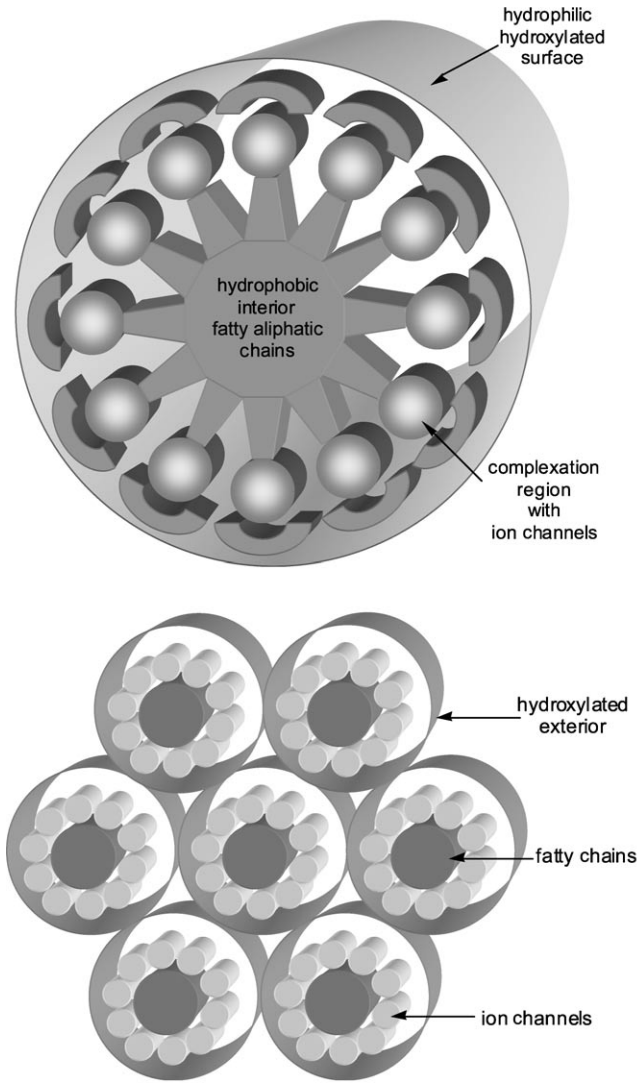

Figure 17. Tubular structure of the hexagonal disordered columnar mesophase.

are towards the interior of the column, whereas the carbohydrate head groups are located at the surfaces of the columns. This is the reverse arrangement for thermotropic

liquid crystalline columnar phases normally found in carbohydrate systems, where the aliphatic chains are usually located at the surfaces of the columns.

The structuring with the sugar groups at the exterior of the columns leads to the possibility of ion channels being formed within the columns and along the column axes.

Our X-ray diffraction studies also show that there is organization of the molecules in the amorphous liquid prior to the phase transition to the liquid crystal state.

Acknowledgements

This work was in part achieved in the former Béghin-Say, CNRS research facility in Villeurbanne (CNRS UMR 143). Financial support from these institutions, and a grant from ANRT to V.M., are gratefully acknowledged.

[1] K. Hill, O. Rhode, *Fett/Lipid* **1999**, *101*, (1.S), 25–33.
[2] I. J. A. Baker, B. Matthews, H. Suares, I. Krodkiewska, D. N. Furlong, F. Grieser, C. J. Drummond, *J. Surfactants Deterg.* **2000**, *3*, 1–11.
[3] S. Nakamura, *Informatik* **1997**, *8*, 866–874.
[4] P. Simon, S. Veyrat, P. Piquemal, C. Montastier, V. Goffin, G. E. Pierard, *Cosmetics Toiletries Magazine*, September **1998**, *113*, 69–72.
[5] A. Guerrero, P. Partal, C. Gallegos, *J. Rheol.* **1998**, *42*, 1375–1388.
[6] A.-S. Muller, J. Gagnaire, Y. Queneau, M. Karaoglanian, J.-P. Maitre, A. Bouchu, *Colloids Surf. A* **2002**, *203*, 55–66.
[7] N. Garti, V. Clement, M. Leser, A. Aserin, M. Fanun, *J. Mol. Liq.* **1999**, *80*, 253–296.
[8] M. A. Bolzinger-Thevenin, J. L. Grossiord, M. C. Poelman, *Langmuir* **1999**, *15*, 2307–2315.
[9] M. H. Kabir, M. Ishitobi, H. Kunieda, *Colloid Polym. Sci.* 2002, **280**, 841–847.
[10] S. E. Ebeler, L. M. Breyer, C. E. Walker, *J. Food Sci.* **1986**, *51*, 1276.
[11] B. A. P. Nelen, J. M. Cooper, in *Emulsifiers in Food Technology* (Ed.: R. J. Whitehurst), Blackwell Publishing Ltd, Oxford, **2004**, pp. 131–161.
[12] C. J. Drummond, C. Fong, I. Krodkiewska, B. J. Boyd, I. J. A. Baker, *Surg. Sci. Ser.* **2003**, *114*, 95–128.
[13] M. Ferrer, F. Comelles, F. J. Plou, M. A. Cruces, G. Fuentes, J. L. Parra, A. Ballesteros, *Langmuir* **2002**, *18*, 667–673.
[14] G. Garofalakis, B. S. Murray, *Langmuir* **2002**, *18*, 4764–4774.
[15] G. Garofalakis, B. S. Murray, D. B. Sarney, *J. Colloid Interface Sci.* **2000**, *229*, 391–398.
[16] I. Söderberg, C. J. Drummond, D. N. Furlong, S. Godkin, B. Matthews, *Colloids Surf. A* **1995**, *102*, 91–97.
[17] T. Kawaguchi, T. Hamanaka, Y. Kito, H. Machida, *J. Phys. Chem.* **1991**, *95*, 3837–3846.
[18] Y. Li, S. Zhang, J. Yang, Q. Wang, *Colloids Surf. A* **2004**, *248*, 127–133.
[19] Y. Li, S. Zhang, Q. Wang, J. Yang, *Tenside Surfactants Deterg.* **2004**, *41*, 26–30.
[20] S. Rouimi, C. Schrosch, C. Valentini, S. Vaslin, *Food Hydrocolloids* **2005**, *19*, 467–478.
[21] V. M. Sadtler, M. Guely, P. Marchal, L. Choplin, *J. Colloid Interface Sci.* **2004**, *270*, 270–275.
[22] V. Molinier, B. Fenet, J. Fitremann, A. Bouchu, Y. Queneau, *J. Colloid Interface Sci.* **2005**, *286*, 360–368.
[23] T. Rades, C. C. Müller-Goymann, *Colloid Polym. Sci.* **1997**, *275*, 1169–1178.
[24] C. M. Paleos, D. Tsiourvas, *Curr. Opin. Colloid Interface Sci.* **2001**, *6*, 257–267.
[25] G. A. Jeffrey, L. M. Wingert, *Liq. Cryst.* **1992**, *12*, 179–202.
[26] H. Van Doren, E. Smits, M. Pestman, J. B. F. N. Engberts, R. M. Kellogg, *Chem. Soc. Rev.* **2000**, *29*, 183–199.
[27] R. Auzely-Velty, T. Benvegnu, G. Mackenzie, J. A. Haley, J. W. Goodby, D. Plusquellec, *Carbohydr. Res.* **1998**, *314*, 65–77.
[28] F. Dumoulin, D. Lafont, P. Boullanger, G. Mackenzie, G. H. Mehl, J. W. Goodby, *J. Am. Chem. Soc.* **2002**, *124*, 13737–13748.
[29] B. J. Boyd, C. J. Drummond, I. Krodkiewska, F. Grieser, *Langmuir* **2000**, *16*, 7359–7367.
[30] V. Vill, T. Böcker, J. Thiem, F. Fisher, *Liq. Cryst.* **1989**, *6*, 349–356.
[31] B. Hoffmann, G. Platz, *Curr. Opin. Colloid Interface Sci.* **2001**, *6*, 171–177.
[32] Y. Queneau, J. Gagnaire, J. J. West, G. Mackenzie, J. W. Goodby, *J. Mater. Chem.* **2001**, *11*, 2839–2844.
[33] H. M. Von Minden, K. Brandenburg, U. Seydel, M. H. J. Koch, V. Garamus, R. Willumeit, V. Vill, *Chem. Phys. Lipids* **2000**, *106*, 157–179.
[34] P. Boullanger, *Top. Curr. Chem.* **1997**, *187*, 275–312.
[35] V. Vill, R. Hashim, *Curr. Opin. Colloid Interface Sci.* **2002**, *7*, 395–409.
[36] S. Bottle, I. D. Jenkins, *Chem. Commun.* **1984**, 385.
[37] I. D. Jenkins, M. B. Goren, *Chem. Phys. Lipids* **1986**, *41*, 225–235.
[38] Y. Queneau, J. Fitremann, S. Trombotto, *C. R. Chim.* **2004**, *7*, 177–188.
[39] V. Molinier, J. Fitremann, A. Bouchu, Y. Queneau, *Tetrahedron: Asymmetry* **2004**, *15*, 1753–1762.
[40] S. Thévenet, A. Wernicke, S. Belniak, G. Descotes, A. Bouchu, Y. Queneau, *Carbohydr. Res.* **1999**, *318*, 52–66.
[41] V. Molinier, K. Wisniewski, A. Bouchu, J. Fitremann, Y. Queneau, *J. Carbohydr. Chem.* **2003**, *22*, 657–669.
[42] S. Riva, J. Chopineau, A. P. G. Kieboom, A. M. Klibanov, *J. Am. Chem. Soc.* **1988**, *110*, 584–589.
[43] G. Carrea, S. Riva, F. Secundo, B. Danieli, *J. Chem. Soc. Perkin Trans. 1* **1989**, 1057–1061.
[44] P. Potier, A. Bouchu, G. Descotes, Y. Queneau, *Tetrahedron Lett.* **2000**, *41*, 3597–3600.
[45] P. Potier, A. Bouchu, J. Gagnaire, Y. Queneau, *Tetrahedron: Asymmetry* **2001**, *12*, 2409–2419.
[46] T. Polat, H. G. Bazin, R. J. Linhardt, *J. Carbohydr. Chem.* **1997**, *16*, 1319–1325.
[47] K. Baczko, C. Nugier-Chauvin, J. Banoub, P. Thibault, D. Plusquellec, *Carbohydr. Res.* **1995**, *269*, 79–88.
[48] C. Chauvin, D. Plusquellec, *Tetrahedron Lett.* **1991**, *32*, 3495–3498.
[49] CRC Handbook of Physics and Chemistry (Ed.: R. C. Priest), CRC Press, Boca Raton, 68th ed., **1988**.
[50] G. W. Gray, J. W. Goodby, *Smectic Liquid Crystals—Textures and Structures*, Leonard Hill, Glasgow and London, **1984**, ISBN 0-249-44168-3; J. W. Goodby, A. J. Slaney, K. Takatoh, Phase Identification and Defect Textures in Liquid Crystals, in *Japanese Handbook of Liquid Crystals* (Ed.: T. Kato), pp. 117–142, **2000**; J. W. Goodby, Microscopy—Applications, Liquid Crystals, in *Encyclopedia of Analytical Chemistry* (Eds.: A. Townshend, P. J. Worsfold, S. J. Haswell, H. W. Werner, I. D. Wilson), Academic Press, London, **2005**, pp. 74–84.
[51] C. H. du Penhoat, S. B. Engelsen, D. Plusquellec, S. Pérez, *Carbohydr. Res.* **1998**, *305*, 131–145.

Received: July 5, 2005
Revised: October 25, 2005
Published online: March 3, 2006

